

The hidden unstable orbits of maps with gaps

Mike R. Jeffrey & Simon Webber*

October 15, 2019

Abstract

Piecewise-continuous maps consist of smooth branches separated by jumps, i.e. isolated discontinuities. They appear not to be constrained by the same rules that come with being continuous or differentiable, able to exhibit period incrementing and period adding bifurcations in which branches of attractors seem to appear ‘out of nowhere’, and able to break the rule that ‘period three implies chaos’. We will show here that piecewise maps are not actually so free of the rules governing their continuous cousins, once they are recognised as containing numerous unstable orbits that can only be found by explicitly including the ‘gap’ in the map’s definition. The addition of these ‘hidden’ orbits — which possess an iterate that lies on the discontinuity — bring the theory of piecewise-continuous maps closer to continuous maps. They restore the connections between branches of stable periodic orbits that are missing if the gap is not fully accounted for, showing that stability changes must occur in discontinuous maps via stability changes not so different to smooth maps, and bringing piecewise maps back under the powerful umbrella of Sharkovskii’s theorem. Hidden orbits are also vital for understanding what happens if the discontinuity is smoothed out to render the map continuous and/or differentiable.

*Department of Engineering Mathematics, University of Bristol, Merchant Venturer’s Building, Bristol BS8 1UB, UK

1 Introduction

Discontinuous maps have been studied extensively from different motivations over the last half century. They have been of interest for their novel bifurcations and robust chaos, which occur in forms not seen in continuous or differentiable maps. Nevertheless there remain literal gaps in our understanding of their periodic attractors — gaps that we shall see here are filled by unstable orbits. Those orbits have remained ‘hidden’ from view because they involve iterates that lie on the map’s discontinuity.

Discontinuous — or more precisely piecewise-continuous — maps, commonly occur when integrating through a flow from some surface to another (or a surface back to itself), when unreachable parts of the flow create gaps in the map’s image. Figures 1-2 illustrate examples in return maps for two-dimensional flows. An early example of a discontinuous map arose with the Lorenz semi-flow [19, 37], which is an abstraction of Lorenz’s famous chaotic flow [30]. Another is the Cherry flow [31, 34, 38], in which the unstable manifolds from a saddlepoint split apart a flow on a torus. In each case the return map to a typical section taken through the flow contains a discontinuity, as sketched in fig. 1.

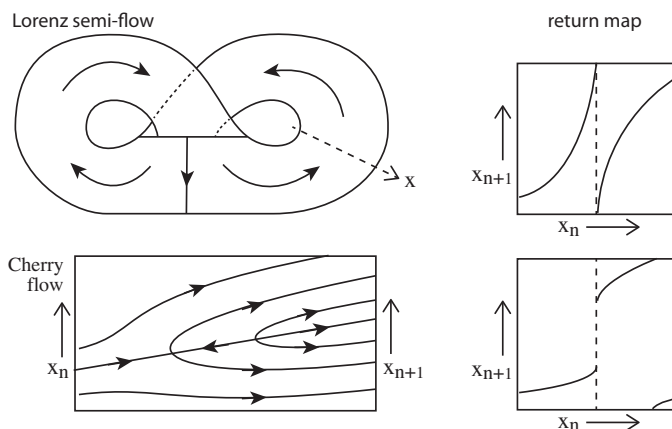


Figure 1: Sources of maps with gaps from saddle-like flows: the Lorenz semi-flow (top) and Cherry flow on the torus (bottom). Example return maps are sketched on the right.

More recently such maps have undergone a resurgence in interest as they appear in growing numbers of electronic, mechanical, and biological applications. These typically involve gaps arising due to a flow that grazes a surfaces of discontinuity, often an impact or frictional sticking surface, an

electronic control surface, see e.g. [10, 25, 32], or a switching thresholds in a sleep-wake cycle [8] or in cell mitosis [24], as sketched in fig. 2.

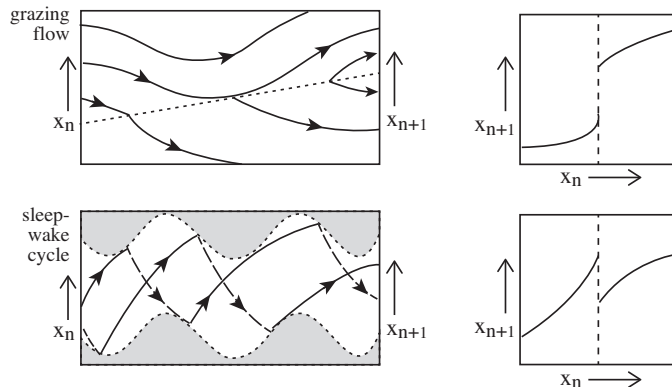


Figure 2: Sources of maps with gaps from grazing flows: tangency to a switching surface in a vector field (top) and to oscillating switching thresholds in a sleep-wake cycle. Example return maps are sketched on the right.

A defining feature of discontinuous maps is that they are seemingly able to display period incrementing or period adding cascades, like that in fig. 3(i), which, with jumps between different branches of attractors, stand in stark contrast to the continuous patterns of period doubling cascades more commonly found in differentiable maps, like that in fig. 3(ii).

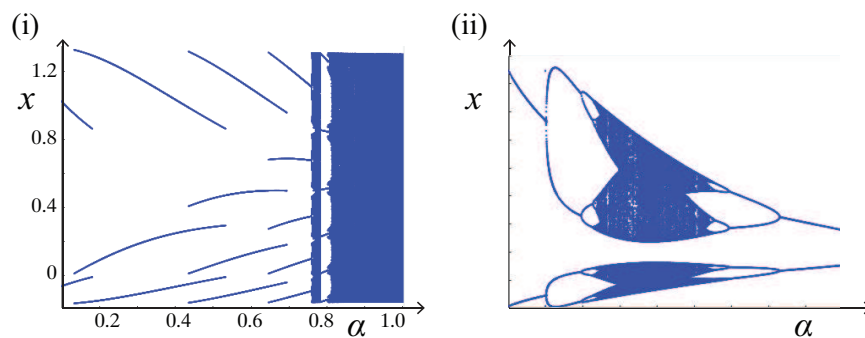


Figure 3: Typical bifurcation diagrams showing periodic orbits and chaos in: (i) a *map with a gap*, (ii) a differentiable map, obtained by numerical ‘shooting’. In (i) the period increases incrementally as α increases until giving way to chaos, in (ii) the period doubles in an infinite cascade towards chaos. The maps generating these are given in section 2 and section 7.

A key feature of period doubling is the uniform scaling with which a doubling cascades lead to chaos, characterized by Feigenbaum’s constants

[13]. By contrast, a period incrementing cascade like fig. 3(i) can typically jump abruptly from any finite period to chaos (a jump from a period 5 to chaos is visible at $\alpha \approx 0.75$ in fig. 3(i)), and while scalings are known for specific maps they have no universal values like Feigenbaum's constants.

A more precise observation is that Sharkovskii's theorem [36] applies only to continuous one dimensional maps on an interval. This theorem has important implications, such as the existence of a period three orbit implying the existence of orbits of all periods (or 'period three implies chaos' [28]), or Coppel's result [11] (a precursor to Sharkovskii) which implies that a continuous map with orbits of period higher than one must have an orbit of period two. A readable short summary and references can be found in [9]. The presence of a discontinuity in the map entirely unravels all of these results (uncontentiously since they are formulated only for continuous maps), or so it seems if we omit the discontinuity from our analysis.

In this article we want to ask why discontinuous maps are permitted to exhibit such behaviours, and foremost *where do the all the missing periodic orbits go*, in the presence of a discontinuity?

We shall show that the key lies not in the property of continuity of a map as such, but in the property of instability. Instability is a big player in a discontinuous map, but in ways that are not often discussed. In short the discontinuity constitutes an infinitely steep change in a map, making it highly unstable there. If there were to exist orbits with iterates on the discontinuity, they would therefore be highly unstable.

Although the regions of periodicity and chaos in diagrams like fig. 3(i) are well understood, the role that instability plays in curtailing regions of periodicity is seldom discussed. The reason that the abrupt jump to chaos happens in fig. 3(i) is that the domains of stability of attractors shrink more quickly than their domains of existence, leaving expanses of parameter space where there exist only unstable orbits, which on the invariant interval \mathcal{I} necessarily result in chaos. Neglecting unstable objects in the map, if there are any that have indeed been neglected, therefore seems obstructive to a complete understanding.

The discontinuity itself receives scant attention in key studies, for example see [15, 16, 20, 26, 29], and at first this seems a natural omission, because the map has no unique well-defined value there. The understanding of periodic orbits, chaos, and bifurcations from these works are extensive (and entirely correct – given the definition of the map as excluding the gap), but in hindsight raise the question of whether something is missing from their dynamical structure. In that hindsight, it will seem strange to have excluded the discontinuity at all. We will show why the discontinuity, and orbits with

iterates lying on it, are crucial to consider, and no less sensible than iterates in regions where a map is well-defined. By revealing ‘missing’ or ‘hidden’ dynamics we mean to show how unexpectedly easy it is to include the gap explicitly in the definition of the map, to make sense of iterates inside it, and to discover the dynamics they generate.

For wider discussion of period adding and incrementing, and other bifurcations of nonsmooth maps, see e.g. [6, 18, 29, 5] and references therein. A starting point for various other applications, history, and fundamental theory can be found in [12, 17].

Our scheme in this paper will be to explicitly include the discontinuity as a set-valued branch of a map, in such a way that orbits are able to have (possibly many) iterates lying on the discontinuity. We describe such orbits as *hidden* in the sense that they evade our view until we consider iterates inside the gap, much as objects behind a curtain remain hidden until we peer behind it, or as square roots of negative numbers appear ‘imaginary’ viewed from the real line; the term ‘hidden’ is also borrowed from similar attempts to reveal the obscure dynamics of ‘flows with a gap’, or *piecewise-smooth flows* [22, 23]).

Our purpose is to establish the principle of the existence of hidden orbits and the role they play. To this end we consider only a simple example of a one-dimensional piecewise linear map with a gap, leaving the tasks of exploring the full role of hidden orbits in stability and bifurcations, and in nonlinear and higher dimensional maps, to future work. We introduce the *map with a gap* in section 2. In section 3 we describe how we handle the discontinuity. Section 4 describes the known periodic orbits, and section 5 introduces the previously undescribed orbits necessary to make sense of the map’s periodic structures, then we relate these to Sharkovskii’s theorem in section 6. We consider how this relates to differentiable maps in section 7, and propose further directions of study along with some final remarks in section 8.

2 The map with a gap

Consider the piecewise-smooth map

$$x_{n+1} = f(x_n) = \begin{cases} f_+(x_n) & \text{if } x_n > 0, \\ f_-(x_n) & \text{if } x_n < 0, \end{cases} \quad (1a)$$

where

$$f_+(x_n) = \alpha x_n - \mu, \quad (1b)$$

$$f_-(x_n) = \beta x_n - \mu - \lambda, \quad (1c)$$

in terms of real constants α, β, μ , and λ .

This system represents the approximation of a map of the form (1a) in the neighbourhood of a discontinuity at $x_n = 0$, where $f(x)$ and $\frac{d}{dx}f(x)$ are finite as $x \rightarrow 0$, but f takes different values as x approaches 0 from the right and left. The piecewise-linear map (1) is known as the ‘*map with a gap*’ (see [12, 20]).

Being piecewise-linear, the solutions of (1) can be written explicitly. The constant λ that creates the gap can be scaled to ± 1 or 0 without loss of generality. Here it will be enough to consider constants of values

$$\beta < 0 < \alpha < 1, \quad \mu > 0, \quad \lambda = -1, \quad (2)$$

giving the map sketched in fig. 4.

For ease of illustration this map will be our sole concern here. This provides some of the richer dynamics of this class of maps (see [12, 20] for more generality), and will allow us to illustrate the appearance of ‘hidden’ unstable orbits associated with the discontinuity. The principle we establish concerning the description of the gap and the orbits it generates can be extended to maps with more gaps, more dimensions, and with nonlinear dependence on x , for instance by generalizing our results on symbolic orbit sequences, the key point of which in the inclusion of the discontinuity or ‘gap’ in any symbol sequence. The map (1) with (2), however, will be enough to establish our point.

For these parameters the interval $-\mu \leq x \leq -\beta\mu - \mu - \lambda$ is invariant, bounded by the first two iterates of 0, namely $f_-(0) = -\mu$ and $f_+(f_-(0)) = -\beta\mu - \mu - \lambda$.

Lemma 2.1. *In the map (1) the interval*

$$\mathcal{I} = \{x : -\mu \leq x \leq -(\beta + 1)\mu - \lambda\}$$

is invariant and attracting.

Proof. Since f_- is strictly positive, every $x_n < 0$ maps into $x_n > 0$. In particular, every x_n on $-\mu \leq x_n \leq 0$ maps to $-\mu - \lambda \leq x_{n+1} \leq -(\beta + 1)\mu - \lambda$. Since f_+ is strictly decreasing, every $x_n > 0$ eventually maps to some $x_{n+m} < 0$ on the interval $f_+(0) = -\mu < x_{n+m} < 0$, which we

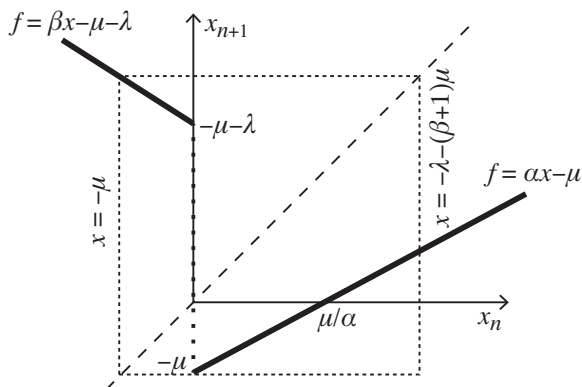


Figure 4: the map

showed then maps back into $x > 0$ with $x_{n+m+1} \leq -(\beta + 1)\mu - \lambda$. So every orbit must pass through $-\mu \leq x_n \leq 0$, and is then constrained inside $-\mu \leq x_n \leq -(\beta + 1)\mu - \lambda$. \square

In the more general language of maps, the interval \mathcal{I} is *locally eventually onto*, implying the existence of either periodic or chaotic attractors on \mathcal{I} . The standard results on the *map with a gap* concern these attractors. The known orbits are those with one iterate on the left branch of the map ($x < 0$) and one or more on the right ($x > 0$). Many orbits of this kind are possible, but they are clearly organised by period incrementing bifurcations and changes of stability, giving the branches of periodic orbits seen, for example, in fig. 3(i). Their existence and stability for general parameter values are well known, giving by stability diagrams like fig. 5. Although this does include unstable orbits, we will show that a large family of unstable orbits are missing.

It will be useful to define a function

$$\mathcal{S}_p(\alpha) := \sum_{k=0}^{p-1} \alpha^k . \quad (3)$$

The p^{th} right iterate $f_+^p(x_n)$ or p^{th} left iterate $f_-^p(x_n)$ are given by the functions

$$f_+^p(x_n) := \alpha^p x_n - \mu \mathcal{S}_p(\alpha) , \quad (4a)$$

$$f_-^p(x_n) := \beta^p x_n - (\mu + \lambda) \mathcal{S}_p(\beta) . \quad (4b)$$

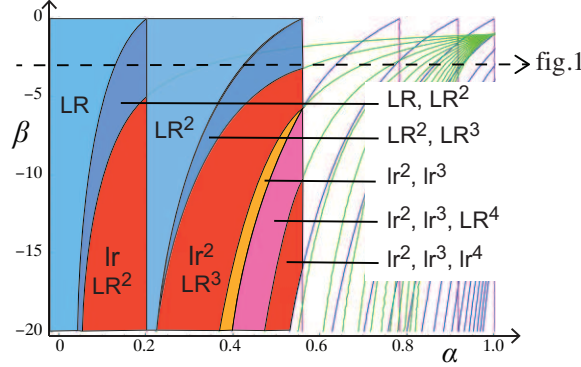


Figure 5: Stability diagram for the *map with a gap*, showing regions of existence of stable or unstable orbits (shaded for the first few zones); $\underline{\mathbf{R}}$ and $\underline{\mathbf{L}}$ denotes right and left iterates of stable orbits, with lower case indicating unstable orbits. This replicates standard results from e.g. [12, 20]. Plotted for $\mu = 1/6$, $\lambda = -1$.

The inverse map is given by

$$x_{n-1} = v(x) = \begin{cases} v_+(x_n) & \text{if } x_n > 0, \\ v_-(x_n) & \text{if } x_n < 0, \end{cases} \quad (5a)$$

where v is a multi-valued function such that $v(f(x)) = x$, with

$$v_+(x_n) = (x_n + \mu)/\alpha, \quad v_-(x_n) = (x_n + \mu + \lambda)/\beta. \quad (5b)$$

The p^{th} inverse right or left iterates (i.e. p^{th} iterates of v_{\pm}) are given by the functions

$$v_+^p(x_n) := \alpha^{-p}x_n + \mu\alpha^{-p}\mathcal{S}_p(\alpha), \quad (6a)$$

$$v_-^p(x_n) := \beta^{-p}x_n + (\mu + \lambda)\beta^{-p}\mathcal{S}_p(\beta). \quad (6b)$$

We will denote an iterate of the map by $\underline{\mathbf{R}}$ if it lies in $x > 0$ and $\underline{\mathbf{L}}$ if it lies in $x < 0$. For iterates lying on periodic orbits, a capital $\underline{\mathbf{R}}$ or $\underline{\mathbf{L}}$ denotes that the orbit is stable, a small $\underline{\mathbf{r}}$ or $\underline{\mathbf{l}}$ denotes that the orbit is unstable. Unlike previous studies we will also consider iterates that lie in the gap (i.e. on the discontinuity) at $x = 0$, and denote these with an $\underline{\mathbf{o}}$ (noting that these will always lie on unstable orbits due to the infinite gradient at the discontinuity).

3 The ‘gap’

We need to decide how to deal with iterates of the map that lie on the discontinuity at $x = 0$. Omitting points inside the gap has not prevented

deep study of the map's bifurcations in previous investigations, but the omission is neither necessary nor ultimately beneficial.

In many works the map's value is left undefined at the gap, such as in [18, 20, 21]. For definiteness some authors select a particular value for $f(0)$, often either the left or righthand limit, $f(0) = f_-(0)$ or $f(0) = f_+(0)$, as in [6, 12, 27], while in [29] both limits are admitted. In studying a logistic-like piecewise-quadratic map in [7], the midpoint of the gap is chosen, $f(0) = \frac{1}{2}(f_-(0) + f_+(0))$, yet to complete the resulting period doubling bifurcation diagram the authors actually admit also the left and right limits, $f(0) = f_-(0)$ and $f(0) = f_+(0)$, and thus find unstable orbits with iterates on the discontinuity. Those unstable orbits are special cases of the orbits we shall find here, and play a similar role in completing gaps in the bifurcation diagram. In [7] it appears that taking special values for the value of the map at the gap (its midpoint and extremities) is sufficient due to the map's symmetry, but here we will need more generality.

Rather than choosing any particular value between $f_-(0)$ and $f_+(0)$ (or indeed outside this range), it is more useful in general to acknowledge that there is *no* definite value for $f(0)$, and build this into our analysis by letting $f(0)$ be set-valued. This follows the philosophy of Filippov's successful approach [14] to piecewise-smooth flows.

We can make the graph of $f(x)$ a continuous curve, albeit with $f(x)$ being set-valued at $x = 0$, by letting $f(0)$ be a continuous set containing $f_{\pm}(0)$. That is, we add to (1a) the equation

$$\begin{aligned} x_{n+1} \in f_0 \quad \text{if } x_n = 0, \\ \text{where } f_0 \supseteq [f_-(x_n), f_+(x_n)]. \end{aligned} \tag{7}$$

This corresponds to drawing a continuous vertical line that joins the vertical axis intercepts at $x_{n+1} = -\mu$ and $x_{n+1} = -\mu - \lambda$ in fig. 4. The inverse at $x = 0$ is

$$x_{n-1} = v_0(x_n) \equiv 0 \quad \text{if } x_n \in f_0. \tag{8}$$

The minimal version of this, in the sense that $x_n = 0$ maps to the smallest possible set of values (interpolating between $(x_n, x_{n+1}) = (0, -\mu)$ and $(0, -\mu - \lambda)$), is given by reducing (7) to

$$x_{n+1} \in f_0 = [f_-(x_n), f_+(x_n)] \quad \text{if } x_n = 0, \tag{9}$$

This is the case we will study here, though all of our results carry to the more general case, with the possibility that there may exist additional unstable

orbits if $f_0 \supset [f_-(x_n), f_+(x_n)]$ (when the vertical branch at $x_n = 0$ extends outside the two vertical axis intercepts in fig. 4).

As a side remark to return to in section 7, one way to handle discontinuities is to consider them as singular limits of smooth functions. In the case of (1) we can consider a map

$$x_{n+1} = F_k(x_n) = f(x_n) + \mathcal{O}(1/k) ,$$

where f is the function (1), while F_k is a continuous and r -times differentiable function for some $r \geq 0$ and $k > 0$, such that

$$\text{for } |x_n| > 1/k , \quad \lim_{k \rightarrow \infty} F_k(x_n) = f_{\pm}(x_n) , \quad (10a)$$

$$\text{for } |x_n| \leq 1/k , \quad \lim_{k \rightarrow \infty} F_k(x_n) \in f_0 . \quad (10b)$$

Thus as $k \rightarrow \infty$, a single-valued branch of $F_k(x)$ tends to infinite gradient as it interpolates between $F_k(-1/k)$ and $F_k(+1/k)$, and so forms the set $f(0)$. We will explore this interpretation in section 7, showing that the unstable orbits hidden by the discontinuity persist for finite k .

4 Orbits of the form $\underline{\text{LR}}^p$ or $\underline{\text{lr}}^p$

The well known periodic orbits of the *map with a gap* (1) take the form of one left iterate and p right iterates, with p being any natural number. Let us review these simple results from [12, 20]. We write such an orbit as $\underline{\text{LR}}^p$ if it is stable and $\underline{\text{lr}}^p$ if it is unstable.

A periodic orbit $\underline{\text{LR}}^p$ or $\underline{\text{lr}}^p$ is a fixed point of the map $x_* = f_+^p(f_-(x_*))$ (using the functions f_- from (1c) and f_+^p from (4a)), or some permutation thereof. It is useful to consider the iterates nearest the gap, given by

$$x_{*L} = f_+^p(f_L(x_{*L})) \quad \text{and} \quad x_{*R} = f_+^{p-1}(f_L(f_+(x_{*R}))) . \quad (11)$$

Their solutions are

$$\frac{\alpha^p(\mu + \lambda) + \mu \mathcal{S}_p(\alpha)}{\beta \alpha^p - 1} < 0 < \frac{\alpha^{p-1}(\beta \mu + \lambda) + \mu \mathcal{S}_p(\alpha)}{\beta \alpha^p - 1} . \quad (12)$$

The inequalities in (12) state that the left iterate must lie in $x < 0$ and the right iterate in $x > 0$. Thus (12) defines the domains of existence of these $\underline{\text{LR}}^p$ or $\underline{\text{lr}}^p$ type orbits. Because they have one left iterate and p right iterates, their stability is simply given by

$$\frac{d}{dx} f_-(f_+^p(x)) = \beta \alpha^p . \quad (13)$$

Therefore, since $\beta < 0 < \alpha$, these constitute stable $\underline{\text{LR}}^p$ orbits for $\beta\alpha^p > -1$, and unstable lr^p orbits for $\beta\alpha^p < -1$.

A bifurcation diagram showing the stable $\underline{\text{LR}}^p$ orbits as α varies, obtained by numerical shooting, is shown in fig. 3(i). In fig. 6 we re-plot this analytically, using the conditions (12) to find the range of α values over which each branch of period $p+1$ orbits exists, and using (13) to show their change of stability as $\beta\alpha^p$ passes through -1 .

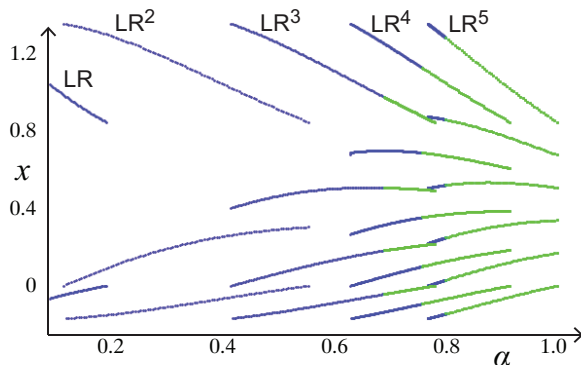


Figure 6: Bifurcation diagram showing branches of periodic orbits of type $\underline{\text{LR}}^p$ (blue) or $\underline{\text{LR}}^p$ (green). In all cases the two lowest branches are the curves of x_{*L} and x_{*R} iterates.

5 Orbits of the form $\underline{\text{or}}^p$ and $\underline{\text{or}}^q \text{lr}^p$

Let us first observe that by including the gap as part of the map in section 3, the point $x = 0$ has become an unstable fixed point for the parameter values $0 < \mu < -\lambda$, denoted as a trivial orbit $\underline{\text{o}}$. (This fixed point will not exist more generally when $-\mu$ and $-\mu - \lambda$ both have the same sign, but this will not prevent the existence of orbits with period greater than one containing an ' $\underline{\text{o}}$ ' iterate).

There are numerous other periodic orbits that contain the point $x = 0$. These can be considered as homoclinic to the fixed point.

Lemma 5.1 (Hidden unstable orbits). *The map with a gap exhibits periodic orbits of the form $\underline{\text{or}}^p$ and $\underline{\text{or}}^q \text{lr}^p$ for $1 \leq q \leq p$. For a set of parameters satisfying (2) the maximum period of these orbits increases with α such that:*

1. *if there exists an orbit of the form $\underline{\text{or}}^p$, then all orbits of the form $\underline{\text{or}}^a$ exist for $1 \leq a \leq p$.*

2. if there exists an orbit of the form $\underline{\text{or}}^q \underline{\text{lr}}^p$, then all orbits of the form $\underline{\text{or}}^p \underline{\text{lr}}^b$ exist for $1 \leq b \leq q$.

Proof. Taking the equations (1), we will show below that the map $x_p = f_+^p(f_0(x_0))$ has a non-trivial fixed point at $x_0 = x_p = 0$, and similarly the map $x_{p+q+1} = f_+^p(f_-(f_+^q(f_0(x_0))))$ has a non-trivial fixed point at $x_0 = x_{p+q+1} = 0$, for certain values of p and q . These fixed points are non-trivial periodic orbits of the map (1), whose other iterates can be found by iterating (1) and (7) from the initial value $x_0 = 0$. Examples of these periodic orbits are shown for a few different values of α in fig. 7 and fig. 8.

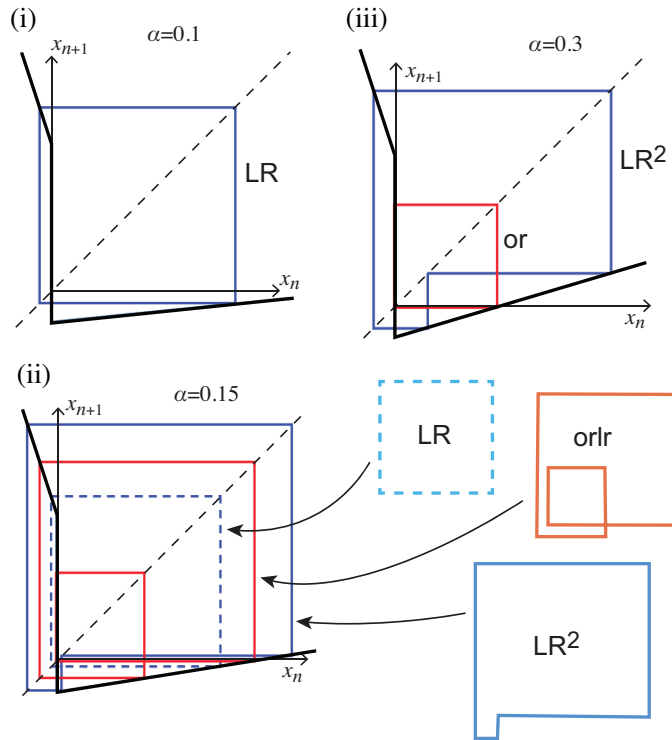


Figure 7: Periodic orbits of the map with a gap, showing the function $f(x_n)$ and its orbits at parameter values $\beta = -3$, $\mu = 1/6$, $\lambda = -1$, with: (i) $\alpha = 0.1$ exhibiting a stable period two $\underline{\text{LR}}$ orbit; (ii) $\alpha = 0.15$ exhibiting a stable period three $\underline{\text{LR}}^2$ orbit and an unstable period four $\underline{\text{orlr}}$ orbit, coexisting with the stable period two $\underline{\text{LR}}$ orbit, with separate images of the three orbits; (iii) $\alpha = 0.3$ exhibiting a stable period three $\underline{\text{LR}}^2$ orbit and an unstable period four $\underline{\text{or}}$ orbit. (Stable orbits shown in blue, unstable orbits in red. We omit the scales for clarity, but they can be inferred from fig. 6 and fig. 9).

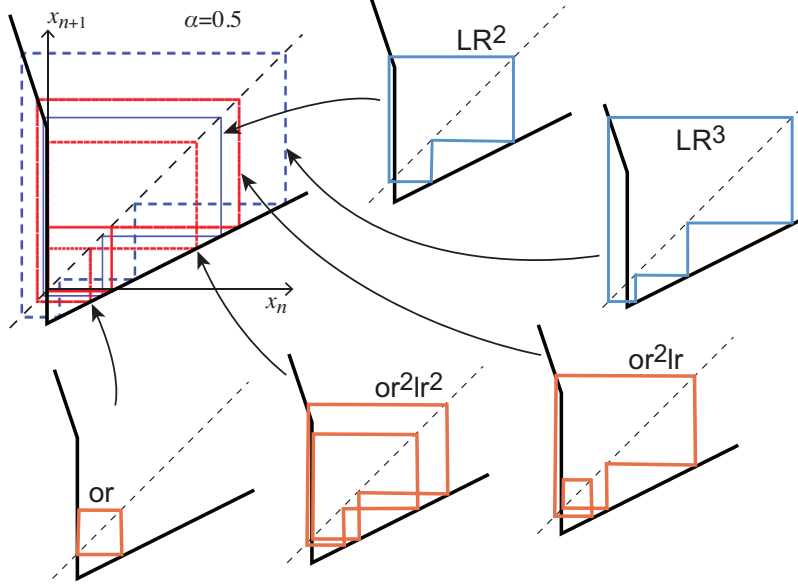


Figure 8: Periodic orbits of the *map with a gap*, showing the function $f(x_n)$ and its orbits at parameter values $\beta = -3$, $\mu = 1/6$, $\lambda = -1$, with $\alpha = 0.5$. Five co-existing orbits are shown in the main figure (top-left), and the other plots show these individually: (reading clockwise) a stable period three $\underline{\text{LR}}^2$ orbit, a stable period three $\underline{\text{LR}}^3$ orbit, an unstable period five orlr^2 orbit, an unstable period six or^2lr^2 orbit, and an unstable period two or orbit. (Stable orbits shown in blue, unstable orbits in red).

Because f_0 is set-valued, it is easier to use the inverse of f , given by (5) and (8), and study the fixed point of the inverse map $x_p = v_0(v_+^p(x_0))$ at $x_0 = x_p = 0$, and of the inverse map $x_{p+q+1} = v_0(v_+^q(v_-(v_+^p(x_0))))$ at $x_0 = x_{p+q+1} = 0$, using the functions (5), (6), and (8).

1. *Orbits of the form or^p .* Assume that $x_{*p} = x_{*0} = 0$ is a fixed point of the map $x_p = v_0(v_+^p(x_0))$. Iterating (5) with (8), the leftmost iterate of this periodic orbit is simply $x_{*1} = \mu/\alpha$, and the rightmost iterate is given by

$$x_{*p} = \frac{\mu}{\alpha^p} \mathcal{S}_p(\alpha). \quad (14)$$

To form a periodic orbit, x_{*p} must map under (8) onto $x_{*p+1} = x_{*0} = 0$, which requires

$$\frac{\mu}{\alpha^p} \mathcal{S}_p(\alpha) \leq -\mu - \lambda. \quad (15)$$

This constitutes the existence criterion for a periodic orbit with rightmost iterate (14) for a given p . Since $\mu > 0$ and $\alpha > 0$ by (2), the function $\frac{\mu}{\alpha^p} \mathcal{S}_p(\alpha)$ is increasing with p , so that for a given α we have

$$\frac{\mu}{\alpha} \mathcal{S}_1(\alpha) < \frac{\mu}{\alpha^2} \mathcal{S}_2(\alpha) < \dots < \frac{\mu}{\alpha^p} \mathcal{S}_p(\alpha) \leq -\mu - \lambda, \quad (16)$$

therefore if a periodic orbit of type $\underline{\text{or}}^p$ exists, the condition (15) implies that periodic orbits of type $\underline{\text{or}}^a$ exist for all $a = 1, \dots, p$.

2. *Orbits of the form $\underline{\text{or}}^q | r^p$.* This is similar to the previous case. Assume that $x_{*p+q+1} = x_{*0} = 0$ is a fixed point of the map $x_{p+q+1} = v_0(v_+^q(v_-(v_+^p(x_0))))$. Iterating (5) with (8), the leftmost iterate of this periodic orbit is again $x_{*1} = \mu/\alpha$, while the rightmost iterate is given again by

$$x_{*p} = \frac{\mu}{\alpha^p} \mathcal{S}_p(\alpha), \quad (17)$$

but if this violates (15), the solution will map under (5) back into $x < 0$. To map back into $x > 0$ this iterate x_{*p} must lie inside the invariant interval \mathcal{I} , hence $x_{*p} < f_-(f_+(0))$. Combining this with violating (15) gives

$$-\mu - \lambda \leq \frac{\mu}{\alpha^p} \mathcal{S}_p(\alpha) \leq -\beta\mu - \mu - \lambda. \quad (18)$$

This constitutes the existence criterion for a periodic orbit with rightmost iterate (17) for a given p and q .

Now we require that the iterates $f_+^b(f_-(f_+^p(0)))$ lie in $x > 0$, that is,

$$0 < v_+^q(v_-(\frac{\mu}{\alpha^p} \mathcal{S}_p(\alpha))) < \frac{\mu}{\alpha^p} \mathcal{S}_p(\alpha) \leq -\beta\mu - \mu - \lambda, \quad (19)$$

which expands as

$$\frac{1}{\alpha^q} \left\{ \left(\frac{\mu}{\alpha^p} \mathcal{S}_p(\alpha) + \mu + \lambda \right) / \beta + \mu \mathcal{S}_q(\alpha) \right\} < \frac{\mu}{\alpha^p} \mathcal{S}_p(\alpha) \leq -\beta\mu - \mu - \lambda. \quad (20)$$

Similarly to the previous case, since the function $\frac{1}{\alpha^q} \mathcal{S}_q(\alpha)$ is strictly increasing with q , for a given α we have

$$\begin{aligned} 0 &< \alpha^{-1} \left\{ \left(\frac{\mu}{\alpha^p} \mathcal{S}_p(\alpha) + \mu + \lambda \right) / \beta + \mu \mathcal{S}_1(\alpha) \right\} \\ &< \alpha^{-2} \left\{ \left(\frac{\mu}{\alpha^p} \mathcal{S}_p(\alpha) + \mu + \lambda \right) / \beta + \mu \mathcal{S}_2(\alpha) \right\} \\ &< \dots \\ &< \alpha^{-q} \left\{ \left(\frac{\mu}{\alpha^p} \mathcal{S}_p(\alpha) + \mu + \lambda \right) / \beta + \mu \mathcal{S}_q(\alpha) \right\} \\ &< \frac{\mu}{\alpha^p} \mathcal{S}_p(\alpha) \leq -\beta\mu - \mu - \lambda, \end{aligned} \quad (21)$$

therefore if a periodic orbit of type $\underline{or}^q \underline{lr}^p$ exists, the condition (18) implies that periodic orbits of type $\underline{or}^p \underline{lr}^b$ exist for all $b = 1, \dots, q$. \square

Figure 9 shows the theoretical iterates of these unstable orbits homoclinic to $x = 0$, given by (14) and (17) and their iterations under the map. They are shown overlaid with the well known orbits of form \underline{LR}^p or \underline{lr}^p from section 4.

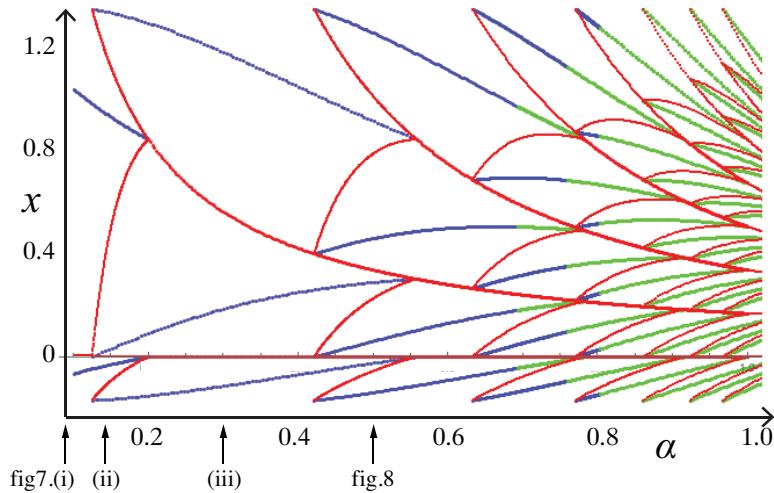


Figure 9: Stable and unstable orbits of the *map with a gap*, including unstable orbits homoclinic to the gap. (Stable \underline{LR}^p orbits shown in blue, unstable \underline{lr}^p orbits in green, unstable $\underline{or}^q \underline{lr}^p$ orbits in red).

This reveals that what appear to be unbalanced appearance and disappearances of periodic orbits are, in fact, bifurcations that are qualitatively similar to the bifurcations familiar from differentiable maps. The curves of attractors and repellers in fig. 9 (and similar diagrams for other parameters, but we show just the one example here) meet in fold-like annihilations of stable/unstable branches, or in pitchfork-like meetings of one stable and two unstable branches producing a single unstable branch. For example, at $\alpha \approx 0.2$ the four branches of an unstable period four \underline{orlr} orbit, and two branches of a stable period two \underline{LR} orbit, collide in a pitchfork-like fashion to produce an unstable period two \underline{or} orbit (the \underline{LR}^2 orbit plays no part in the bifurcation).

The precise shape of the curves in fig. 9, for instance their local growth rates with the bifurcation parameter, are nevertheless markedly different from differentiable maps. Clearly the precise forms of these bifurcations

deserves further study, and this is already underway, but as is common in maps (or similarly in flows) with discontinuities, the task is a lengthy one. The lack of continuity prevents all systems capable of exhibiting any given bifurcation being reduced to a single topological normal form. Instead, many normal forms will be required to represent the different instances of folds (and pitchforks, cusps, etc.) in maps with distinct topologies. This is obviously beyond our scope here.

As we come to understand these bifurcations in more detail, we will then be able to understand more precisely their relation to differentiable maps. To give some hints in this direction we show in section 7 how objects corresponding to hidden orbits persist in a continuous or differentiable map, and at the end of the paper we look briefly at what happens to the bifurcation diagram fig. 6 as we transition between a map that is discontinuous and one that is differentiable.

What fig. 9 shows is that orbits with iterates in the gap play an important role. Whether or not we regard them to be sensible orbits in any strict sense, their significance lies in organising the surrounding dynamics and bifurcations, in particular ensuring that stable or unstable orbits do not pop arbitrarily in and out of existence without branches of unstable hidden orbits appearing to balance any changes of existence or stability.

6 Reviving Sharkovskii

Since the unstable orbits of the forms \underline{or}^p and $\underline{or}^q \underline{lr}^p$ are homoclinic to the fixed point, they can be concatenated in infinitely many ways to form orbits of higher period. Thus, including the fixed point \underline{o} , if there exist orbits of type

$$\underline{o}, \quad \underline{or}^{s_i}, \quad \text{and} \quad \underline{or}^{q_j} \underline{lr}^{p_k},$$

for some sets of integers, $s_1, s_2, \dots, q_1, q_2, \dots, p_1, p_2, \dots$, then there also exist orbits whose sequences are any arbitrary concatenation of these. Since the unit-length sequence \underline{o} is included in this, orbits of any higher period can be formed, consistent with the outcome of Sharkovskii's theorem [36].

Take the three cases in fig. 7:

- (i) There exists a stable period two \underline{LR} orbit. If Sharkovskii's theorem did apply then there should also exist a fixed point, which is provided by the unstable point \underline{o} where the vertical branch crosses the diagonal.
- (ii) The standard theory reveals stable orbits of period two, \underline{LR} , and period three, \underline{LR}^2 . If Sharkovskii's theorem did apply then it would imply the

existence of orbits of all periods. A non-trivial period four orbit, \underline{orlr} , is indeed found, along with the unstable fixed point \underline{o} . All other periods result from concatenations of these.

- (iii) The standard theory reveals a stable orbit of period three \underline{LR}^2 . Again if Sharkovskii's theorem did apply then it would imply the existence of orbits of all periods. A period two orbit, \underline{or} , is found in this case, along with the unstable fixed point \underline{o} , and all other periods result from concatenations of these.

Though the concatenations in (ii) and (iii) seem somewhat trivial, as they all overlap via the homoclinic connection to \underline{o} , nonetheless they generate unique symbol sequences of all periods. Their existence restores Sharkovskii's result, albeit in a rather degenerate fashion.

More general maps might not have a fixed point \underline{o} , but still possess higher period hidden orbits with an iterate \underline{o} on the discontinuity, and our conjecture is that these will similarly ensure the satisfaction of Sharkovskii's theorem. This does, of course, remain to be proven, and we make further remarks in section 8.

The result becomes particularly meaningful when we seek to relate discontinuous maps to their continuous counterparts — which must satisfy Sharkovskii's theorem — in the next section.

7 Smoothing the map – bringing the ‘gap’ to life

Are hidden orbits, with an iterate on the gap, in any way real and meaningful, or are they mere figments of taking the map to be set-valued at the gap? Besides their role in bifurcation diagrams like fig. 9, or in extending Sharkovskii's theorem in section 5, there is another, perhaps more direct way to see that hidden orbits are realisable, and that is by smoothing the map.

A device that has long been used to remove some of the conceptual uncertainties of dealing with a discontinuity is to represent the jump as the (singular) limit of a continuous or differentiable process. A map with a discontinuity at some point $x = \xi$, say

$$x_{n+1} = f(x_n) \quad \text{with} \quad \lim_{k \rightarrow \infty} f(x \pm \frac{1}{k}) = f_{\pm}(\xi), \quad (22)$$

can be made continuous by introducing some monotonic branch $f_0(x)$ in $|x - \xi| \leq 1/k$ such that $x_{n+1} = f_0(x_n)$, with the map unchanged for $|x - \xi| >$

$1/k$. If we call the new map $x_{n+1} = F_k(x)$ then it must obey

$$x_{n+1} = F_k(x_n) \quad \text{such that} \quad \lim_{k \rightarrow \infty} F_k(x_n) = f(x_n), \quad (23)$$

where $F_k(x)$ is r -times differentiable in x for some $r \geq 0$.

We will show a couple of examples here to illustrate how the orbits from section 5 persist, remaining as unstable periodic orbits still close to, but no longer homoclinic to, the map's fixed point. The *map with a gap* is unimodal, and if we take k sufficiently small then it begins to resemble a tent map (if made continuous piecewise-linear) or a logistic map (if made differentiable).

The simplest continuous ($r = 0$) example is a piecewise map, such as

$$x_{n+1} = \begin{cases} f_+(x_n) & \text{if } kx_n > +\frac{1}{2}, \\ f_0(x_n) & \text{if } k|x_n| \leq \frac{1}{2}, \\ f_-(x_n) & \text{if } kx_n < -\frac{1}{2}, \end{cases} \quad (24a)$$

where

$$f_0(x_n) = \left(\frac{1}{2} + kx_n\right)f_+(x_n) + \left(\frac{1}{2} - kx_n\right)f_-(x_n). \quad (24b)$$

In fig. 10 we use this to regularize the map for the parameters in fig. 7(ii), showing the first few periodic orbits.

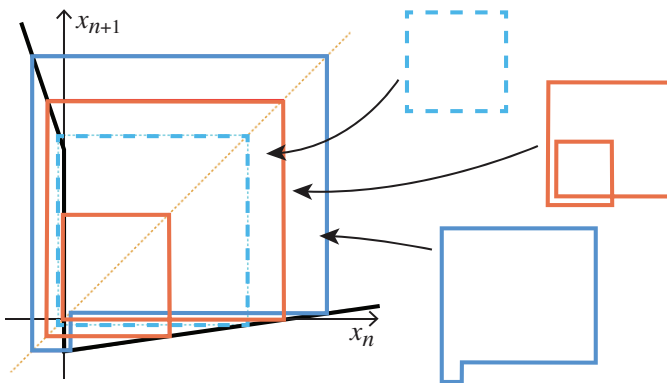


Figure 10: Piecewise-linear continuous approximation of fig. 7(ii), with $\beta = -3$, $\mu = 1/6$, $\lambda = -1$, $\alpha = 0.15$, and $k = 84$. The periodic orbits of type LR, LR², and orlr, are clearly identifiable.

An example of a differentiable map ($r \geq 1$) is given by

$$x_{n+1} = \frac{1+\phi_k(x_n)}{2}f_+(x_n) + \frac{1-\phi_k(x_n)}{2}f_-(x_n), \quad (25a)$$

where $\phi_k(x)$ is any differentiable sigmoid function and $k > 0$, such that $\frac{d}{dx}\phi_k(x) > 0$ for $k|x| < 1$ and

$$\lim_{k \rightarrow \infty} \phi_k(x_n) = \text{sign}(x_n). \quad (25b)$$

In fig. 11 we use this to smooth the map for the parameters in fig. 7(ii), again showing the first few periodic orbits.

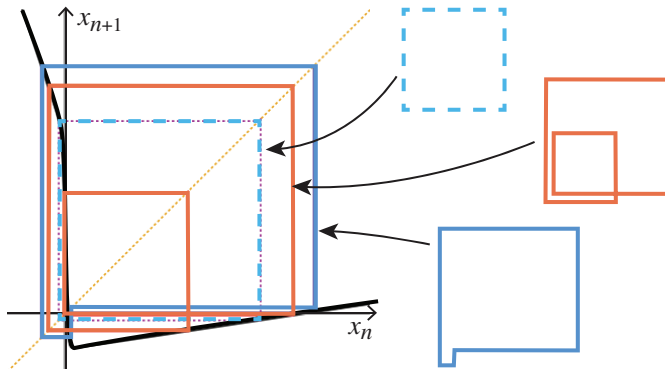


Figure 11: Analytic approximation of fig. 7(ii), taking $\phi_k(x) = \tanh(kx)$ with $\beta = -3$, $\mu = 1/6$, $\lambda = -1$, $\alpha = 0.15$, and $k = 84$. The periodic orbits of type $\underline{\text{LR}}$, $\underline{\text{LR}}^2$, and $\underline{\text{orlr}}$, are clearly identifiable.

As $k \rightarrow \infty$, the systems (24) and (25) each tend to the *map with a gap* as defined by (1) and (9). The point $x = 0$ then maps to the whole interval between $f_+(0)$ and $f_-(0)$, consistent with our inclusion of the gap as set-valued in (9).

The persistence of the $\underline{\text{LR}}$ and $\underline{\text{LR}}^2$ stable orbits, and the $\underline{\text{orlr}}$ unstable orbit, can be clearly seen in both figures 10 and 11, where $\underline{\text{o}}$ now denotes an iterate on the branch of the map with gradient of order k . Numerous other stable and unstable periodic orbits can also be found with iterates crowded closely to the $\underline{\text{orlr}}$ orbit (not shown), and indeed since Sharkovskii's theorem now holds there must be infinitely many such orbits.

Ultimately, as we let $k \rightarrow \infty$, these infinitely many orbits must go somewhere. What one observes is that they crowd up until, when k becomes infinite and the map becomes discontinuous, they lie on top of each other as homoclinic orbits to the unstable fixed point, consistent with our results from section 5 to section 6, providing an interpretation of overlapping concatenations of hidden orbits as the singular limits in which many unstable orbits of a continuous map crowd together.

8 Closing Remarks

Although Sharkovskii’s theorem does not strictly apply to a map with a discontinuity, by considering the map to be set-valued across the gap we essentially restore continuity (albeit in a set-valued sense), and recover Sharkovskii’s result. This suggests that Sharkovskii’s theorem might be extended to discontinuous maps by amending its proof to permit a set-valued function.

If the existence of these unstable orbits has come to light in combinatoric literature, then the authors are not yet aware of such a result, and they have not come to light in recent work from the perspective of discrete dynamical theory. Differential inclusions — which can be used to study ‘flows with a gap’ (i.e. *piecewise-smooth flows*) — have been studied in literature attempting to extend Sharkovskii’s theorem to ordinary differential equations [2, 33, 1, 3, 4], and it is possible that hidden orbits may form part of the picture in those cases too by applying the ideas of [22, 23] which introduced the notion of *hidden dynamics* more generally.

Unstable orbits are, of course, harder to pinpoint in numerical analyses than stable orbits. Their role in connecting period doubling cascades in differentiable maps was considered in [35]. Here we have shown that unstable orbits can be identified with iterates lying on a discontinuity, and these help make sense of the bifurcation structures of discontinuous maps, showing how closely they fit with intuition learned from continuous maps.

We have only shown an example of orbits passing through the gap, and left a more general theory to future work. It is tempting to consider other particular cases, for example the obvious counter-example to Sharkovskii’s theorem,

$$x_{n+1} = \begin{cases} x_n + 1 & \text{if } x_n < 2, \\ x_n - 2 & \text{if } x_n \geq 2, \end{cases} \quad (26)$$

on the interval $0 \leq x < 3$, in which every iterate seemingly has period three, lying on an orbit with one right and two left iterates, and so these orbits are null-stable. Clearly this violates Sharkovskii’s result as no other periods exist. If we include the gap, however, then immediately there exists an unstable fixed point \underline{o} where the vertical branch intersects the diagonal, and also a period two orbit $\underline{o}\underline{l}$. Thus we have periods 1, 2, and 3, and orbits of all periods are formed through concatenations of these, and although they overlap in x -space, they have unique $\underline{o}, \underline{l}, \underline{r}$ symbol sequences.

So let us return to the question of whether hidden orbits to be interpreted as real objects, and whether values inside the gap should be interpreted as

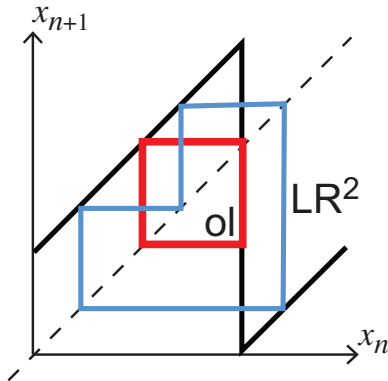


Figure 12: A simple counter-example seeming to contain only orbits of period three. An example period three orbit is shown, along with the hidden period two orbit that restores Sharkovskii's result.

valid iterates of a map. In section 7 we saw that hidden orbits correspond to perfectly regular, though highly unstable, orbits of a nearby continuous map. But the significance of the gap and its hidden orbits does not rely on such interpretations. In the case of the Cherry or Lorenz flows in fig. 1, hidden orbits of the map would not correspond to any actual orbits of the original flows. Dynamical attractors and repellers do not have to represent valid states to have a role as organising centers of local or global dynamics, to organize bifurcations in diagrams like fig. 9, or as described in section 5, to permit the extension of results like Sharkovskii's theorem.

To illustrate, consider a model of a population x that varies as $\frac{dx}{dt} = a - bx^2$. As a model this has at most one fixed point, at $x = \sqrt{b/a}$ when $b/a > 0$. But regardless of the domain of x , mathematically the equation $\frac{dx}{dt} = a - bx^2$ always has two fixed points at $x = \pm\sqrt{b/a}$. Their existence reveals itself in the dynamics, influencing the population in $x > 0$, even though they do not correspond to anything physical generally since it does not make sense to consider 'negative' or 'imaginary' populations. Similarly, 'hidden' orbits have a dynamical role, whether or not they are part of the original application or of the chosen definition of the map. Whether points inside the gap can be visited by the state of a given system will depend on the application, and this determines whether hidden orbits represent realisable physical dynamics.

The qualitative difference between continuous and discontinuous maps is not so great as it once appeared, provided the discontinuity is adequately described. Hidden orbits mean that many of our insights of continuous maps

seem also to apply to those with jumps. By learning more about the difference between the qualitative dynamics of discontinuous versus continuous maps, we can also learn better how to use discontinuities to approximate steep branches in nonlinear maps, without losing qualitative features crucial to the dynamics.

Having smoothed the map in section 7, it is interesting to go one step further, and ask how the bifurcation diagram in fig. 3(i) arises from the more familiar period doubling cascades as in fig. 3(ii) as a differentiable map limits to a discontinuous one. The branches of unstable or^p and $\text{or}^q \text{lr}^p$ orbits in section 5 reveal that period incrementing occurs via saddle-node like births of pairs of stable and unstable periodic orbits. Still, these and the stable branches in fig. 3(i) must be associated with periodic windows somewhere among the chaos of fig. 3(ii). An analytic understanding has not been reached yet, but let us conclude with some numerical observations to guide future study.

In fig. 13 we present a sequence of bifurcation diagrams for the map (25), showing how its dynamics changes from very large k to small k .

For $k = 1000$ there is no clear difference from the bifurcation diagram for the *map with a gap* in fig. 3(i). As k decreases to around 70, the overlap between different branches decreases, shrinking the regions of coexistence of different periods. As these branches continue to retract they leave a gap, which is filled by chaos as seen at $k = 60$. The chaotic regions widen and period doubling cascades become apparent. By $k = 20$ we can see that, as the chaotic regions continue to widen and eventually merge, the periodic branches will shrink into small periodic windows.

As we continue to decrease k the higher periods leave the parameter region in the diagram, but we can observe closely what happens to the period 3 branch. The single chaotic band that still exists for $k = 11$ at around $\alpha \approx 0.6$ splits into three bands, and disappear by $k = 8$. This period 3 window then rapidly closes between $k \approx 7.74$ and $k \approx 7.73$, leaving behind a familiar period doubling cascade, that merely continues to warp and give way to period doubling as we decrease to around $k = 4$ and beyond.

The key images in fig. 13 are perhaps those showing the transition from $k \approx 7.74$ to $k \approx 7.73$, which reveal how the periodic branches of the incrementing cascade for the very stiff (large k) or discontinuous map, are associated with periodic windows of familiar chaos delimited by period doubling cascades. The particular window is not obvious at smaller k . The steep nonlinearity created as k increases warps the chaotic region, and effectively rips open these chaotic windows as k increases, or, put another way, the near-discontinuous map hops through the chaotic region between

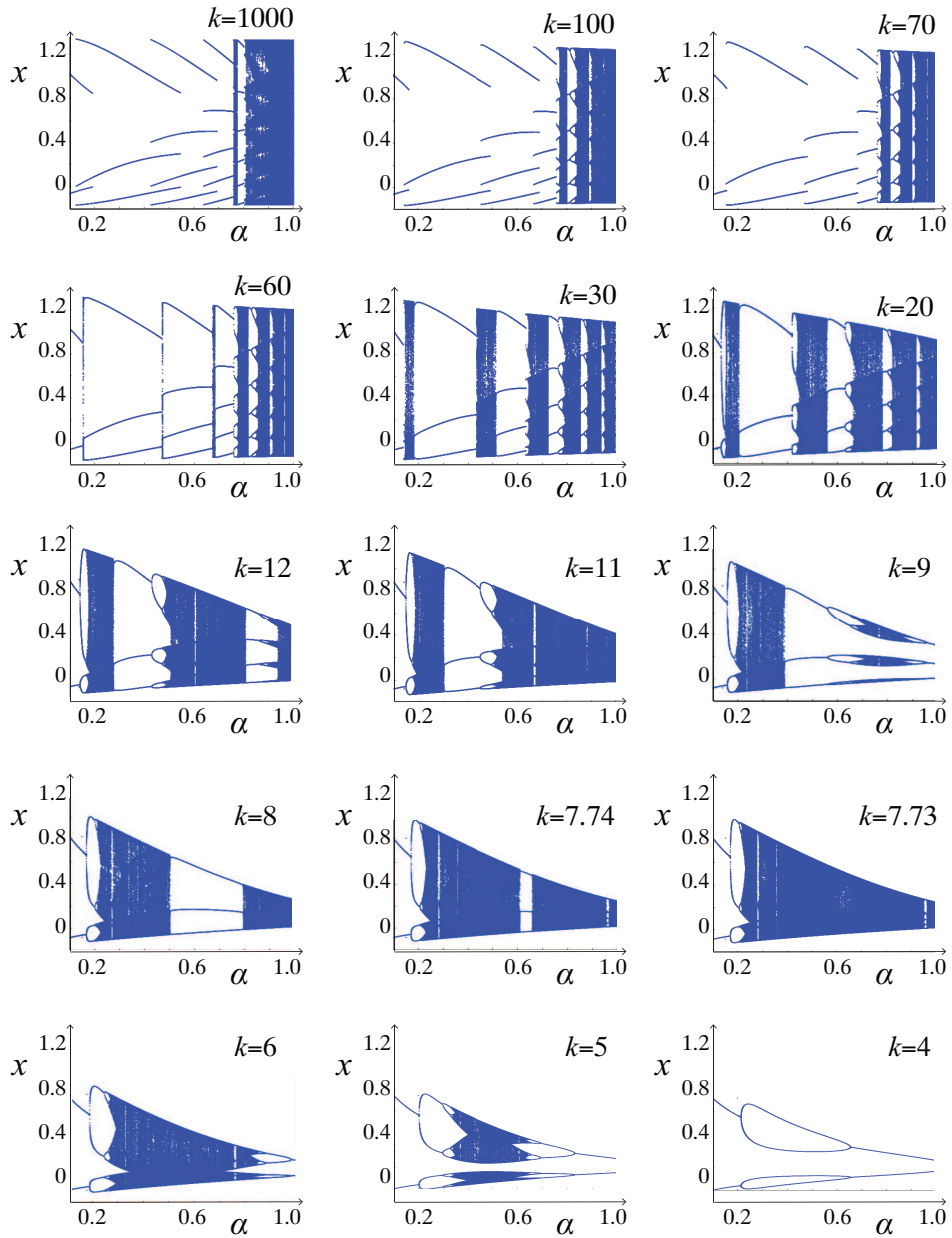


Figure 13: Bifurcation diagram obtained for analytic map (25), taking $\phi_k(x) = \tanh(kx)$ with $\beta = -3$, $\mu = 1/6$, $\lambda = -1$, comparable to fig. 3 and fig. 9. The stiffness k is as shown in each diagram. Obtained by numerical shooting, showing stable periodic orbits only.

periodic windows whose periods increase incrementally with α . The steep nonlinearity for large k , and ultimately its infinite gradient at $x = 0$ as $k \rightarrow \infty$ stretches out these periodic windows into sustained branches.

In principle it is possible to include the unstable orbits in these diagrams by means of continuation methods, but this is made more challenging by the stiffness of the map at large k . It is quite easy to see that the orbits studied in section 5 will be taken over by the regions of chaos that appear as k decreases from around $k \approx 70$ to $k \approx 60$.

It would be more interesting to study further why certain periodic windows, near certain parameter values, are picked out from the differentiable map's periodic doubling cascades. It seems likely that this depends greatly on particular type of smoothing function, e.g. (24) or (25), chosen, but a result showing otherwise would be interesting indeed. A careful analysis should reveal why the windows chosen take successively increasing period, since although the reason for this is clear in the discontinuous map, it is not so obvious in the differentiable map.

The features of the bifurcation diagrams in fig. 13 may suggest that there is general interest in more closely studying the dynamics of maps with steep, hence strongly unstable, branches. Those features persist whether the map is continuous or not, and are instead associated with whether the function is Lipschitz continuous, that is whether $|f(x_1) - f(x_2)| \leq L|x_1 - x_2|$ for some constant L , and it may be of interest to study whether there is a determinable magnitude of L that determines whether a map will exhibit period incrementing or period doubling.

In this paper we have taken a piecewise linear map with a single gap as an example, merely to establish the principle that any gap, in any map with any number of discontinuities in any number of dimensions and any degree of nonlinearity, may exhibit hidden orbits. This leaves much to be understood about their role in such more general circumstances.

References

- [1] J. Andres, J. Fiser, and L. Jüttner. On a multivalued version of the Sharkovskii theorem and its application to differential inclusions. *Set-Valued Analysis*, 10:1–14, 2002.
- [2] J. Andres, T. Fürst, and K. Pastor. Sharkovskii's theorem, differential inclusions, and beyond. *Top. Meth. Non. Anal.*, 33:149–68, 2009.

- [3] J. Andres, L. Jüttner, and K. Pastor. On a multivalued version of the Sharkovskii theorem and its application to differential inclusions ii. *Set-Valued Analysis*, 13:47–68, 2005.
- [4] J. Andres and K. Pastor. On a multivalued version of the Sharkovskii theorem and its application to differential inclusions iii. *Top. Meth. Non. Anal.*, 22:369–86, 2003.
- [5] V. Avrutin, L. Gardini, I. Sushko, and F. Tramantona. *Continuous and Discontinuous Piecewise-Smooth One-Dimensional Maps*, volume 95 of *Nonlinear Science Series A*. World Scientific, 2019.
- [6] V. Avrutin, A. Granados, and M. Schanz. Sufficient conditions for a period incrementing big bang bifurcation in one-dimensional maps. *Nonlinearity*, 24:2575–98, 2011.
- [7] V. Avrutin and M. Schanz. Period-doubling scenario without flip bifurcations in a one-dimensional map. *IJBC*, 15(4):1267–84, 2005.
- [8] M. P. Bailey, G. Derks, and A. C. Skeldon. Circle maps with gaps: Understanding the dynamics of the two-process model for sleep–wake regulation. *European Journal of Applied Mathematics*, 29(5):845–68, 2018.
- [9] Keith Burns and Boris Hasselblatt Source. The Sharkovsky Theorem: A natural direct proof. *The American Mathematical Monthly*, 118(3):229–44, 2011.
- [10] W. Chin, E. Ott, H. E. Nusse, and C. Grebogi. Grazing bifurcations in impact oscillators. *Phys. Rev. E*, 50(6):4427–4444, Dec 1994.
- [11] W. A. Coppel. The solution of equations by iteration. *Proc. Cambridge Philos. Soc.*, 51:41–3, 1955.
- [12] M. di Bernardo, C. J. Budd, A. R. Champneys, and P. Kowalczyk. *Piecewise-Smooth Dynamical Systems: Theory and Applications*. Springer, 2008.
- [13] M. J. Feigenbaum. Quantitative universality for a class of non-linear transformations. *J. Stat. Phys.*, 19(1):25–52, 1978.
- [14] A. F. Filippov. *Differential Equations with Discontinuous Righthand Sides*. Kluwer Academic Publ. Dordrecht, 1988 (original in Russian 1985).

- [15] P. Glendinning. Robust new routes to chaos in differential equations. *Physics Letters A*, 168:40–46, 1992.
- [16] P. Glendinning. The anharmonic route to chaos: kneading theory. *Nonlinearity*, 6:349–367, 1993.
- [17] P. Glendinning and M. R. Jeffrey. An introduction to piecewise smooth dynamics. *Advanced Courses in Mathematics – CRM Barcelona (Birkhauser)*, 2019 (in press).
- [18] A. Granados, L. Alsedra, and M. Krupa. The period adding and incrementing bifurcations: From rotation theory to applications. *SIAM Rev.*, 59(2):225–92, 2017.
- [19] J. Guckenheimer and R.F. Williams. Structural stability of Lorenz attractors. *Publ. Math. IHES*, 50:59–72, 1979.
- [20] S. J. Hogan, L. Higham, and T. C. L. Griffin. Dynamics of a piecewise linear map with a gap. *Proc. R. Soc. A*, 463:49–65, 2007.
- [21] P. Jain and S. Banerjee. Border-collision bifurcations in one-dimensional discontinuous maps. *IJBC*, 13(11):3341–51, 2003.
- [22] M. R. Jeffrey. Hidden dynamics in models of discontinuity and switching. *Physica D*, 273-274:34–45, 2014.
- [23] M. R. Jeffrey. *Hidden Dynamics: The mathematics of switches, decisions, & other discontinuous behaviour*. Springer, 2019.
- [24] M. R. Jeffrey and H. Dankowicz. Discontinuity-induced bifurcation cascades in flows and maps with application to models of the yeast cell cycle. *Physica D*, 271:32–47, 2014.
- [25] H. Jiang, A. S. E. Chong, Y. Ueda, and M. Wiercigroch. Grazing-induced bifurcations in impact oscillators with elastic and rigid constraints. *International Journal of Mechanical Sciences*, 127:204–14, 2017.
- [26] J. P. Keener. Chaotic behavior in piecewise continuous difference equations. *Transactions of the American Mathematical Society*, 261(2):589–604, 1980.
- [27] L. E. Kollar, G. Stepan, and J. Turi. Dynamics of piecewise linear discontinuous maps. *Int.J.Bif.Chaos*, 14(7):2341–2351, 2004.

- [28] T-Y. Li and J. A. Yorke. Period three implies chaos. *The American Mathematical Monthly*, 82(10):985–92, 1975.
- [29] T. LoFaro. Period-adding bifurcations in a one parameter family of interval maps. *Mathematical and Computer Modelling*, 24:27–41, 1996.
- [30] E. N. Lorenz. Deterministic nonperiodic flow. *Journal of the Atmospheric Sciences*, 20(2):130–41, 1963.
- [31] M. Martens, S. Van Strien, W. De Melo, and P. Mendes. On Cherry flows. *Ergodic Theory and Dynamical Systems*, 10(3):531–554, 1990.
- [32] A. B. Nordmark. Universal limit mapping in grazing bifurcations. *Phys. Rev. E*, 55:266–270, 1997.
- [33] F. Obersnel and O. Pierpaolo. Period two implies chaos for a class of ODEs. *Proc. Am. Math. Soc.*, 135(7):2055–8, 2007.
- [34] J. Palis and W. de Melo. *Geometric theory of dynamical systems*. Springer-Verlag, 1982.
- [35] E. Sander and J. A. Yorke. Connecting period-doubling cascades to chaos. *IJBC*, 22(2):1250022, 2012.
- [36] A. N. Sharkovskii. Co-existence of cycles of a continuous mapping of the line into itself. *Ukrainian Math. J.*, 16:61–71, 1964.
- [37] R.F. Williams. The structure of Lorenz attractors. *Publ. Math. IHES*, 50:73–99, 1979.
- [38] J. Yang. Cherry flow: physical measures and perturbation theory. *Ergodic Theory and Dynamical Systems*, 37(8):2671–88, 2017.